

# Elimination of the chirp of optical pulses through cascaded nonlinearities in periodically poled lithium niobate waveguides

Sheng Liu,<sup>1</sup> Kwang Jo Lee,<sup>1,\*</sup> Katia Gallo,<sup>2</sup> Periklis Petropoulos,<sup>1</sup> and David J. Richardson<sup>1</sup>

<sup>1</sup>*Optoelectronics Research Centre, University of Southampton, Southampton, SO17 1BJ, United Kingdom*

<sup>2</sup>*Department of Applied Physics, Royal Institute of Technology (KTH), 10691 Stockholm, Sweden*

\*Corresponding author: [kjl@orc.soton.ac.uk](mailto:kjl@orc.soton.ac.uk)

We propose and demonstrate a novel method for the elimination of arbitrary frequency chirp from short optical pulses. The technique is based on the combination of two cascaded second-order nonlinearities in two individual periodically poled lithium niobate waveguides. The proposed scheme operates independently of the spectral phase characteristics of the input pulse, producing a near-transform-limited output.

*OCIS codes:* 060.4510, 130.3730, 190.2620, 190.4410, 230.4320.

Picosecond optical pulses are widely used in diverse applications, such as optical time division-multiplexed communications, optical sensors, and optical imaging systems. Such short optical pulses can be generated using a variety of means including mode-locked lasers, gain-switched laser diodes, and even externally modulated continuous-wave (CW) light sources. However, the

generated optical pulses often have some associated intrinsic frequency chirp and the cumulative effects of dispersion and various optical nonlinearities often experienced during onward transmission in fibre systems can either intensify this chirp, or induce additional nonlinear degradation, leading to compromised performance for many applications.

Suitable lengths of fibre are usually employed to remove the linear chirp component associated with non transform-limited optical pulses and to thereby improve the pulse properties. However, the length of the dispersion compensating fibre has to be matched to the exact chirp characteristics and typically needs to be determined on a case-by-case basis.

In recent years, the use of cascaded second-order nonlinear processes in periodically poled lithium niobate (PPLN) waveguides has attracted considerable interest as a promising route to perform all-optical signal processing [1]. The technology provides for high nonlinear coefficients, an ultra-fast optical response, bit-rate and modulation format transparency, low cross-talk, and no added spontaneous emission noise. Cascaded second-harmonic and difference-frequency generation (cSHG/DFG) and cascaded sum- and difference-frequency generation (cSFG/DFG) have both been exploited in various all-optical signal-processing applications, such as wavelength conversion [2], format conversion [3], logic gates [4], tunable optical time delays [5], and phase sensitive amplification [6].

In this paper, we propose and demonstrate an effective method to remove frequency chirps induced in ps-optical pulses. The technique relies on the generation of a conjugated replica of the input chirped pulse in a first PPLN waveguide via cSHG/DFG, followed by the nonlinear interaction of the two phase-conjugated signals through cSFG/DFG in a second PPLN waveguide: a process which eventually yields chirp-free pulses at the system output. Our scheme

has the distinct advantage that even unknown or nonlinear chirps can be erased without requiring detailed knowledge of the input pulse form, as briefly discussed in the following section.

Figure 1(a) illustrates our scheme for the elimination of chirp in pulses based on the combination of cSHG/DFG and cSFG/DFG in two cascaded PPLN waveguides. The first one performs phase-conjugation ( $A_{cj}=A_{cp}^*$ ) and wavelength conversion (to  $\lambda_{cj}$ ) of the original chirped input pulse [ $A_{cp}(t)$  at  $\lambda_{cp}$ ] by means of cascaded SHG (with a CW pump) and DFG [2]. All of the resulting optical waves after the first PPLN sample are passed through an optical processor. This is a programmable amplitude filter which rejects both the pump and the SH waves, and equalises the optical power of the input pulse with that of its conjugate. Equalization of the intensities of the two signals is required in order to optimise the efficiency of the nonlinear processes in the second PPLN waveguide, where the two pulses interact with each other as two pulsed pumps to generate the sum-frequency (SF) wave. A chirp-free output in the same wavelength band as the two original signals is then generated by DFG interaction between the SF wave and a CW wave (at  $\lambda_{si}$ ) conveniently placed close to the original wavelengths. In a simplified picture (neglecting pump depletion and walk-off) the generated SF field (subsequently mapped back into the telecommunication band via DFG) will be proportional to the modulus squared of the original signal ( $A_{sf} \sim A_{cp}A_{cj} = |A_{cp}|^2$ ), meaning that the imaginary parts of the input field are cancelled out and thus any frequency chirp is erased. To simulate the actual response of the second PPLN stage (also in the presence of pump depletion and group velocity mismatch), we used the following coupled mode equations:

$$\begin{aligned}
\frac{\partial A_{cp}}{\partial z} + \frac{1}{v_1} \frac{\partial A_{cp}}{\partial t} &= -i\Gamma_1 A_{sf} A_{cj}^* \exp(-i\Delta\beta_1 z) \\
\frac{\partial A_{cj}}{\partial z} + \frac{1}{v_2} \frac{\partial A_{cj}}{\partial t} &= -i\Gamma_1 A_{sf} A_{cp}^* \exp(-i\Delta\beta_1 z) \\
\frac{\partial A_{si}}{\partial z} + \frac{1}{v_3} \frac{\partial A_{si}}{\partial t} &= -i\Gamma_2 A_{sf} A_{out}^* \exp(-i\Delta\beta_2 z) \\
\frac{\partial A_{out}}{\partial z} + \frac{1}{v_4} \frac{\partial A_{out}}{\partial t} &= -i\Gamma_3 A_{sf} A_{si}^* \exp(-i\Delta\beta_2 z) \\
\frac{\partial A_{sf}}{\partial z} + \frac{1}{v_5} \frac{\partial A_{sf}}{\partial t} &= -i\Gamma_1 A_{cp} A_{cj} \exp(i\Delta\beta_1 z) - i\Gamma_4 A_{si} A_{out} \exp(i\Delta\beta_2 z),
\end{aligned} \tag{1}$$

where  $A_{cp}$ ,  $A_{cj}$ ,  $A_{sf}$ ,  $A_{si}$ , and  $A_{out}$  denote the slowly varying envelopes of the input chirped pulse, conjugated replica, SF, CW-wave, and chirp-free output waves, respectively. The group velocities ( $v_{cp,cj,sf,si,out}$ ), the nonlinear coupling coefficients ( $\Gamma$ ) and the phase-mismatches ( $\Delta\beta$ ) were calculated as in Ref. [3], with reference to the PPLN waveguide used in our experiments. Numerical simulations based on the full model [Eq. (1)] confirmed the capability of the scheme to remove a broad range of chirp profiles, even in the presence of moderate walk-off between the original and SF signals in the PPLN waveguide. This can be intuitively justified with a semi-analytical approach similar to Ref. [7], in which the output field in the frequency domain is expressed as the product between the PPLN filter function (which depends on the group velocity mismatch between the pumps and the SF) and the Fourier transform of the modulus squared of the input signal [FT $\{|A_{cp}|^2\}$ ]. This yields a response which is insensitive to the phase of the input field. In the simplest case of a spectrally symmetric narrowband signal, the acceptance bandwidth of the process is the same as that of SHG from an “equivalent” un-chirped pump with the same intensity distribution as the input signal (i.e.  $|A_{cp}|$ ). At first approximation, the limitation of the technique originates from the walk-off in the waveguide, which can be estimated as e.g.  $\sim 10$  ps, for Gaussian inputs in a 3cm-long PPLN waveguide (as in our experiments) [7]. Yet even the presence of (moderate) walk-off does not compromise the applicability of the scheme,

as it may induce a broadening of the field profile [with respect to  $|A_{cp}(t)|^2$ ] but no significant chirp at the output, as shown by the simulations in Fig.1 as well as by the experimental results presented in the next section, where phase-removal is performed with pulses shorter than 10 ps (6.5 ps). Nevertheless, increasing the walk-off and/or the pump depletion further do ultimately translate in non-transform-limited outputs (as for SHG in Ref. [8]).

Figure 2 shows the experimental setup used to realise our chirp-free pulse generation system. Two 30-mm-long fibre-pigtailed PPLN waveguides (HC Photonics Corp.) were used for the cSHG/DFG and SFG/DFG steps. Their SHG phase matching wavelength was 1546 nm at 50°C and 42°C, respectively. A CW laser operating at 1546.0 nm was used as the pump for the first PPLN device. 10-GHz, 2-ps pulses generated from a mode locked erbium glass oscillator (ERGO) at 1552 nm were launched into a length of single mode fibre (SMF) to generate the input chirped pulses. The CW pump and the chirped pulses were combined in a 3-dB coupler and then amplified before being launched into the first PPLN waveguide. The total power at the input of the waveguide was restricted to 21 dBm to protect its coupling connectors. Figure 3(a) shows the measured spectrum of the signals at the output of the first PPLN waveguide (pump, chirped input signal and conjugated pulse). The optical signal to noise ratio (OSNR) of the conjugate signal was measured to be 12.2dB. An optical processor (Finisar WaveShaper 4000E) filtered out both the pump and the SH waves, and equalised the optical power of the input chirped pulses with that of the conjugate pulses. The two signals were then amplified and combined with a 1558-nm CW beam in a second 3-dB coupler. All three waves were then launched into the second PPLN waveguide to interact with each other via cSFG/DFG as described in Fig. 1. The resultant spectrum, measured after the second PPLN device, is shown in Fig. 3(b). The measured OSNR of the cSFG/DFG output signal at 1533.7 nm was 14dB, which can be improved by

implementing the PPLN waveguide with higher conversion efficiency available in state-of-the-art PPLN waveguides technology.

In order to assess the performance of the system and its capacity to eliminate the chirp of optical pulses, we performed linear frequency resolved optical gating (*l*-FROG) measurements, using an electro-optic modulator as the sampling gate [9]. Figure 4(a), (c), and (e) shows the spectrograms obtained for the input chirped pulse, its conjugated replica, and the resultant chirp-free output pulse respectively. Normalized intensities and phases of the corresponding retrieved pulses are also shown in Fig. 4(b), (d), and (f). As shown in Fig. 4(a), (b) and (c), (d), the chirp of the conjugated pulses is opposite to that of the original signal, whereas the chirp in the cSFG/DFG signal has been cancelled out to produce a chirp-free output, as can be seen in Fig. 4(e) and (f). The measured chirp rate parameters of the input and output pulses were  $-0.0086 \text{ ps}^{-2}$  and zero within the resolution limit of the FROG, respectively.

The temporal traces of the chirped input and the chirp-free output pulses measured with an optical sampling oscilloscope (OSO, EXFO PSO-100) are shown in Fig. 5(a) and (b). A filter, tunable both in bandwidth and centre wavelength (Alnair Labs.), was used after the second PPLN waveguide to extract and characterise each of the pulse forms separately. The measured pulse widths of each pulse were 6.5 ps and 6.6 ps, respectively. The time-bandwidth product for the chirp-free output was 0.48, which indicates good quality, close to transform-limited pulses.

We have demonstrated an effective method to erase the chirp of ps-long pulses and generate chirp-free output pulses. The technique, which is based on a combination of cascaded nonlinear effects in two different PPLN waveguides, operates independently of the input chirp characteristics and requires only limited knowledge of the input pulse shape.

## Acknowledgement

The research leading to these results has received funding from the UK EPSRC under grant agreement EP/F032218/1 and the European Union FP7 Network of Excellence BONE (Building the Future Optical Network in Europe) (FP7-ICT-2007-1 216863). Katia Gallo gratefully acknowledges support from the EU under grant agreement PIEF-GA-2009-234798.

## References

1. C. Langrock, S. Kumar, J. E. McGeehan, A. E. Willner, and M. M. Fejer, “All-optical signal processing using  $\chi^{(2)}$  nonlinearities in guided-wave devices,” *J. Lightwave Technol.* **24**, 2579–2592 (2006).
2. K. Gallo, G. Assanto, and G. I. Stegeman, “Efficient wavelength shifting over the erbium amplifier bandwidth via cascaded second order processes in lithium niobate waveguides,” *Appl. Phys. Lett.* **71**, 1020–1022 (1997).
3. K. J. Lee, S. Liu, F. Parmigiani, M. Ibsen, P. Petropoulos, K. Gallo, and D. J Richardson, “OTDM to WDM format conversion based on quadratic cascading in a periodically poled lithium niobate waveguide,” *Opt. Express* **18**, 10282–10288 (2010).
4. J. E. McGeehan, M. Giltrelli, and A. E. Willner, “All-optical digital 3-input AND gate using sum- and difference-frequency generation in a PPLN waveguide,” *Electron. Lett.* **43**, 409–410 (2007).
5. Y. Wang, C. Yu, L. Yan, A. E. Willner, R. Roussev, C. Langrock, M. M. Fejer, J. E. Sharping, and A. L. Gaeta, “44-ns continuously tunable dispersionless optical delay element using a PPLN waveguide with two-pump configuration, DCF, and a dispersion compensator,” *IEEE Photon. Technol. Lett.* **19**, 861–863 (2007).

6. K. J. Lee, F. Parmigiani, S. Liu, J. Kakande, P. Petropoulos, K. Gallo, and D. Richardson, “Phase sensitive amplification based on quadratic cascading in a periodically poled lithium niobate waveguide,” *Opt. Express* **17**, 20393–20400 (2009).
7. J. Prawiharjo, K. Gallo, N. G. Broderick, and D. Richardson, “Frequency-resolved optical gating in the 1.55 $\mu$ m band via cascaded  $\chi^{(2)}$  processes”, *J. Opt. Soc. Am, B*, 1985-1993 (2005).
8. J.-F. Campos, Y. Wang, B. Chen, C.-Q Xu, S. Yang, E. Ponomarev, and X. Bao, “40-GHz picosecond pulse generation in a MgO-doped PPLN waveguide”, *J. Lightwave Technol.* **24**, 3698-3708.
9. K. T. Vu, A. Malinowski, M. A. F. Roelens, M. Ibsen, P. Petropoulos, and D. J. Richardson, “Full characterization of low-power picosecond pulses from a gain-switched diode laser using electro-optic modulation-based linear FROG,” *IEEE Photon. Technol. Lett.* **20**, 505–507 (2008).

## Figure captions

Fig. 1. (a) Illustration of chirp elimination in a short pulse based on both cSHG/DFG and cSFG/DFG in two cascaded PPLN waveguides, (b) Normalised powers  $[P(t)/P_{\text{peak}}]$  and phases  $[\varphi]$  of the pumps ( $c_j$  and  $c_p$ , solid and dashed lines, respectively) and the cSFG/DFG output ( $out$ , black dots) of the second PPLN stage, calculated from Eq. (1) for a 3 cm-long PPLN waveguide with a normalised efficiency  $\eta_{\text{nor}}=60\% \text{ W}^{-1}\text{cm}^{-2}$ , with 7 ps-long (FWHM) Gaussian input pump pulses with equalised (peak) powers  $P_{c_p} = P_{c_j} = 30 \text{ mW}$ , at  $\lambda_{c_p}=1540 \text{ nm}$  and  $\lambda_{c_j}=1552 \text{ nm}$ , respectively. CW input signal at  $\lambda_{s_i}=1558 \text{ nm}$ , with  $P_{s_i}= 1 \text{ mW}$ .

Fig. 2. Experimental setup used to generate the chirp-free pulse via a combination of cSHG/DFG and cSFG/DFG. PC: polarization controller, EDFA: erbium-doped fibre amplifier, *l*-FROG: linear frequency resolved optical gating, OSA: optical spectrum analyser.

Fig. 3. Spectral traces measured after (a) the first PPLN waveguide and (b) the second PPLN waveguide.

Fig. 4: Measured FROG traces for (a) the input chirped pulse, (c) its conjugated replica, and (e) the resultant chirp-free output pulses. Retrieved normalized intensities and phase profiles of (b) the input chirped pulse, (d) its conjugated replica, and (f) the resultant chirp-free output pulse.

Fig. 5. Temporal traces of (a) the chirped input and (b) the chirp-free output pulses measured using the optical sampling oscilloscope.

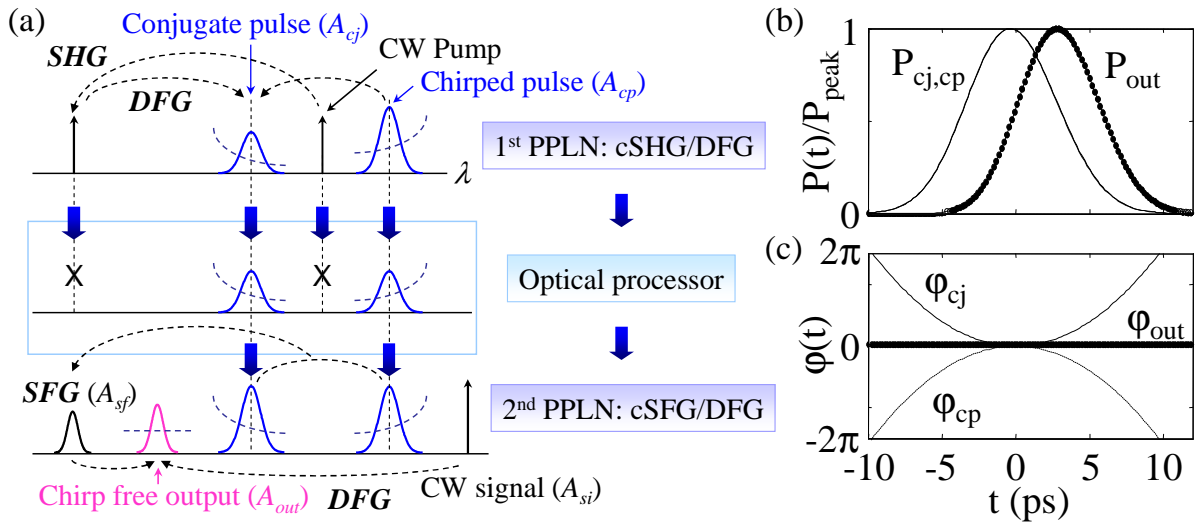


Fig. 1

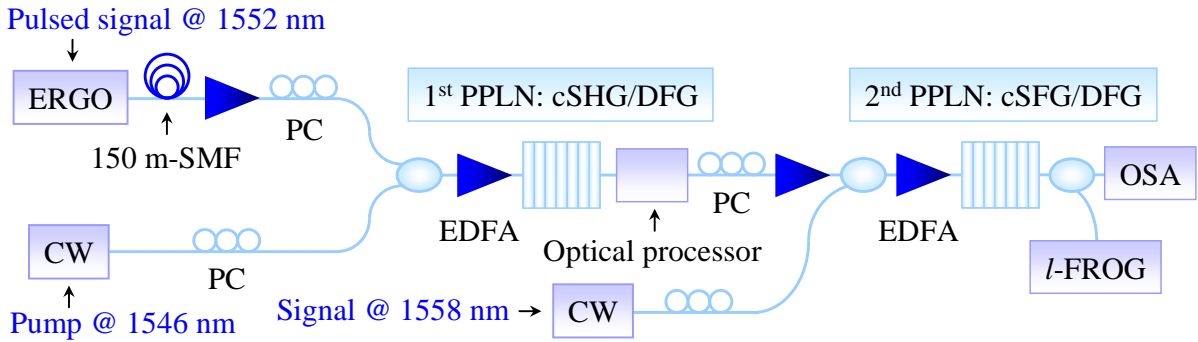


Fig. 2

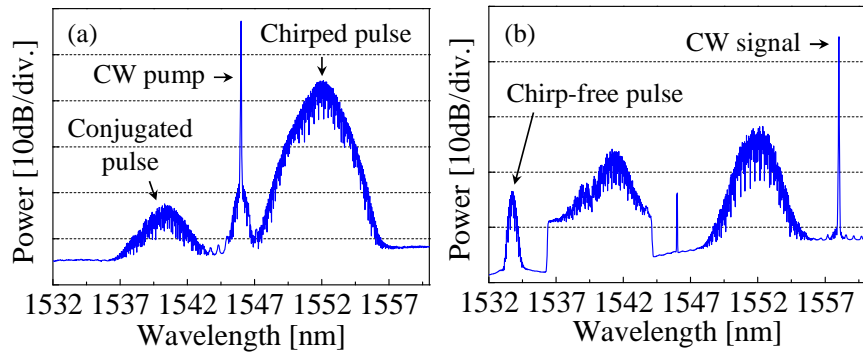


Fig. 3

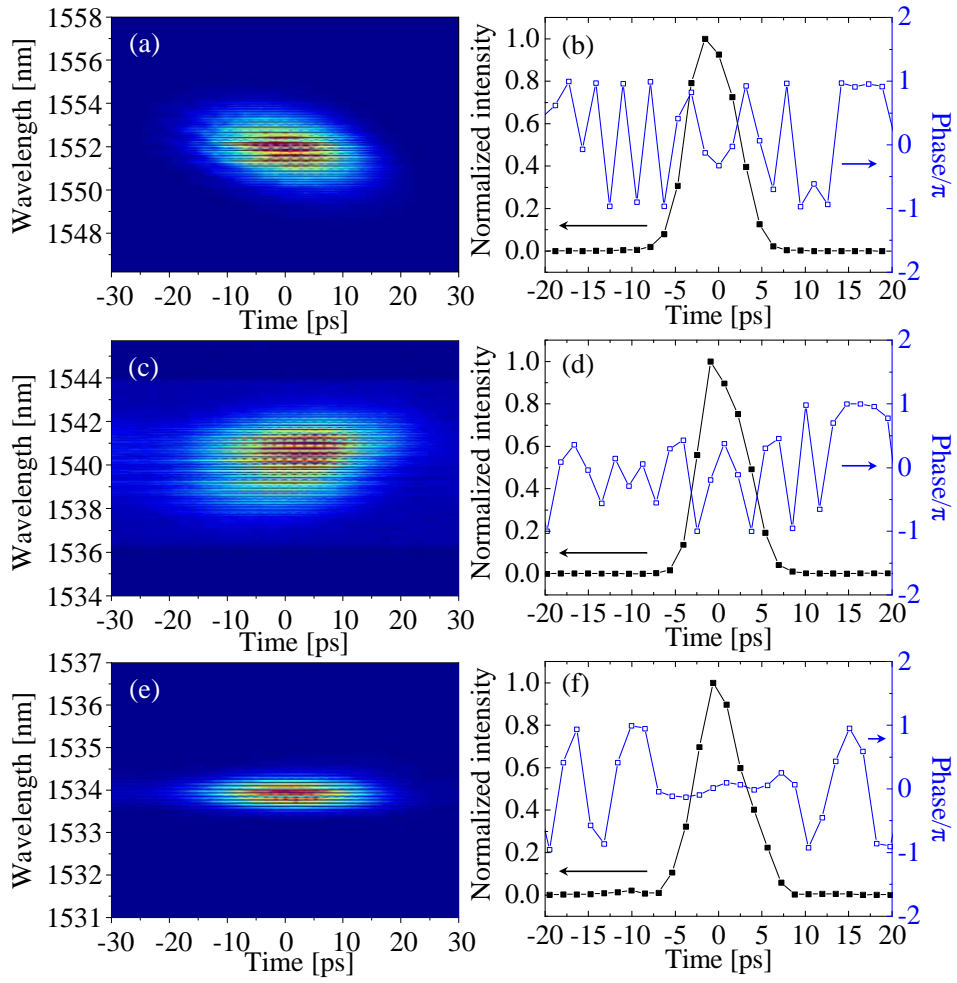


Fig. 4

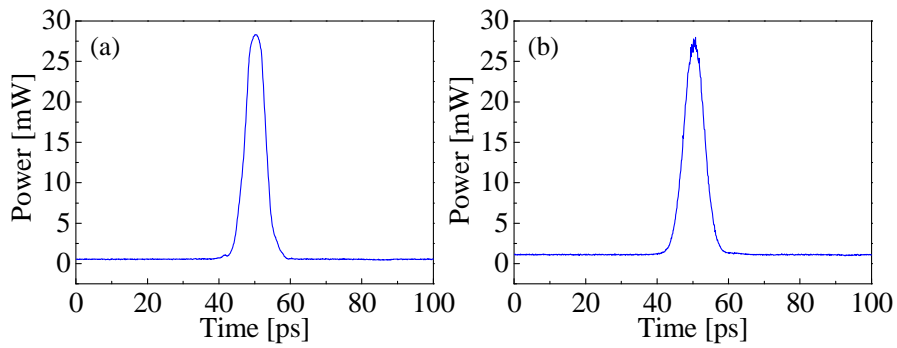


Fig. 5